

# A numerical study of vortex dynamics of flexible wing propulsors

Kartik Venkatraman

Associate Professor

November 23, 2009

Report 2008-2009



Aeroservoelasticity Laboratory

Department of Aerospace Engineering

Indian Institute of Science

Bangalore-560012, India

<b>Report Documentation Page</b>			Form Approved OMB No. 0704-0188	
<p>Public reporting burden for the collection of information is estimated to average 1 hour per response, including the time for reviewing instructions, searching existing data sources, gathering and maintaining the data needed, and completing and reviewing the collection of information. Send comments regarding this burden estimate or any other aspect of this collection of information, including suggestions for reducing this burden, to Washington Headquarters Services, Directorate for Information Operations and Reports, 1215 Jefferson Davis Highway, Suite 1204, Arlington VA 22202-4302. Respondents should be aware that notwithstanding any other provision of law, no person shall be subject to a penalty for failing to comply with a collection of information if it does not display a currently valid OMB control number.</p>				
1. REPORT DATE <b>24 NOV 2009</b>	2. REPORT TYPE <b>Final</b>	3. DATES COVERED <b>11-09-2008 to 10-09-2009</b>		
4. TITLE AND SUBTITLE <b>A numerical study of vortex formation and shedding from flapping flexible wing propulsors</b>			5a. CONTRACT NUMBER <b>FA23860814073</b>	
			5b. GRANT NUMBER	
			5c. PROGRAM ELEMENT NUMBER	
6. AUTHOR(S) <b>Kartik Venkatraman</b>			5d. PROJECT NUMBER	
			5e. TASK NUMBER	
			5f. WORK UNIT NUMBER	
7. PERFORMING ORGANIZATION NAME(S) AND ADDRESS(ES) <b>Indian Institute of Science,,AE 606, Department of Aerospace Engineering,Bangalore 560012,India,IN,560012</b>			8. PERFORMING ORGANIZATION REPORT NUMBER <b>N/A</b>	
9. SPONSORING/MONITORING AGENCY NAME(S) AND ADDRESS(ES) <b>AOARD, UNIT 45002, APO, AP, 96337-5002</b>			10. SPONSOR/MONITOR'S ACRONYM(S) <b>AOARD</b>	
			11. SPONSOR/MONITOR'S REPORT NUMBER(S) <b>AOARD-084073</b>	
12. DISTRIBUTION/AVAILABILITY STATEMENT <b>Approved for public release; distribution unlimited</b>				
13. SUPPLEMENTARY NOTES <b>This work is continued/renewed for the second year in AOARD # 094077</b>				
14. ABSTRACT <b>Results of variation propulsive parameters of flexible foil with and without inertial effects with characteristic frequency are presented. There is considerable difference between the propulsive parameters of flexible foil with and without inertial effects.</b>				
15. SUBJECT TERMS <b>Low Re Aerodynamics, Flexible airfoils, Computational Fluid Dynamics</b>				
16. SECURITY CLASSIFICATION OF:			17. LIMITATION OF ABSTRACT <b>Same as Report (SAR)</b>	18. NUMBER OF PAGES <b>15</b>
a. REPORT <b>unclassified</b>	b. ABSTRACT <b>unclassified</b>	c. THIS PAGE <b>unclassified</b>	19a. NAME OF RESPONSIBLE PERSON	

## Abstract

The dynamic properties such as time dependent pressure loading, speed, free stream velocity, and local acceleration of the hydrofoil determine the instantaneous deformation of the hydrofoil, which has effect on the propulsive characteristics of the aquatic animal. A potential flow analysis is done on the flexible hydrofoil, to evaluate the both inertial and elastic effects on propulsive characteristics such as efficiency and thrust coefficient.

Thrust coefficient and efficiency are characterised with respect to various non-dimensional parameters such as mass ratio and characteristic frequency for heaving, pitching and combined heave-pitch motions. Results are explained with respect to change in shape of the foil and the dynamics of fluid-structure interaction for various values of mass ratio and characteristic frequency. Thrust coefficient and propulsive efficiency increases with increased mass ratio whereas thrust coefficient and propulsive efficiency increases as characteristic frequency decreases. The flexibility is decreased to a lower value such that the ratio of excitation frequency is equal to the second mode natural frequency and the propulsive parameters are plotted with respect to the flexibility parameter characteristic frequency. It is found that the hydrodynamic output obtained is higher than the hydrodynamic input, thus giving propulsive efficiencies more than one for comparatively low characteristic values.

Results of variation propulsive parameters of flexible foil with and without inertial effects with characteristic frequency are presented. There is considerable difference between the propulsive parameters of flexible foil with and without inertial effects.

## Contents

<b>List of figures</b>	iii
<b>List of tables</b>	iv
<b>1. Introduction</b>	1
<b>2. Fluid-structure interaction model</b>	3
2.1. Unsteady inviscid two dimensional airfoil theory	3
2.2. Unsteady incompressible viscous flow	3
2.3. Structural Model	4
<b>3. Results and Discussions</b>	5
3.1. Large amplitude undulatory motion	7
<b>4. Concluding remarks</b>	8
<b>5. Acknowledgement</b>	8

## List of Figures

1	Schematic description of model	3
2	Wake patterns after three cycles of heaving motion for flexible foil.	4
3	Effect of $\omega_c L/U$ on propulsive parameters, $\frac{H}{L} = 0.1$ , $a_1 L/U = 0.000586$ , $\mu = 10$ .	5
4	Influence of inertia and elasticity on instantaneous lift	6
5	Effect of $\omega_c L/U$ on propulsive parameters, $\alpha_0 = 5^\circ$ , $a_1 L/U = 0.000586$ , $\mu = 10$ .	6
6	Wake patterns after three cycles of heaving rigid foil.	6
7	Wake patterns after three cycles of heaving flexible foil.	7
8	Effect of $\mu$ on propulsive parameters, $\frac{H}{L} = 0.1$ , $a_1 L/U = 0.000586$ , $\omega_c L/U = 10$ .	7
9	Effect of $\mu$ on propulsive parameters, $\alpha_0 = 5^\circ$ , $a_1 L/U = 0.000586$ , $\omega_c L/U = 10$ .	8
10	Effect of $\omega_c L/U$ on thrust coefficient, $\frac{H}{L} = 3$ , $\alpha_0 = 5^\circ$ , $a_1 L/U = 0.000586$ , $\mu = 10$ .	9
11	Effect of $\omega_c L/U$ on thrust coefficient, $\frac{H}{L} = 3$ , $\alpha_0 = 5^\circ$ , $a_1 L/U = 0.000586$ , $\mu = 10$ .	9

## List of Tables

1	Non-dimensional parameters	5
---	----------------------------	---

## 1. Introduction

The time dependent pressure loading, free stream velocity, and local displacement, velocity and acceleration of the foil, determine instantaneous response. The dynamic coupling between the hydrofoil and surrounding fluid determines the final lift and thrust force acting on it. Owing to the complexity in modeling the fluid-structure interaction of the flexible airfoil, many researchers have carried the analysis by prescribing the motion of the flexible wing based on experiments (see Mittal *et al.* 2006) or predetermined motion of the flexible wing (see Liu & Bose 1997) to study the flexible effects on the propulsive performance. Pederzani & Haj-Hariri (2006) have analysed the effect of chordwise flexibility on the heaving airfoil.

First and foremost in the study of the propelling hydrofoils is the work of Lighthill (1960). Lighthill (1960) worked out the slender body theory for an aquatic animal, whose dimensions and movements at right angles to its direction of motion are small, while its cross section varies along it only gradually. The flow of the slender body theory consists of the steady flow around the stretched straight body and the flow due to the displacements of the body perpendicular to the direction of motion. The important conclusions of his theory were that the traveling wave down the flexible body is  $5/4^{\text{th}}$  of the desired forward speed and the amplitude increases from zero over the front portion to a maximum at the tail so that the angular recoil is minimised. The boundary layer effects were considered but found to not qualitatively alter the efficiency.

Lighthill (1970) made a quantitative analysis on the locomotion of aquatic vertebrates using slender body theory. He showed how a series of modifications of basic undulatory mode found in aquatic vertebrates tends to improve speed and efficiency. The modifications he found are necking of the anterior to the caudal fin, yawing axis along the trailing edge, and large depth of cross section near the mass center which is needed for low recoil. He used the 2-D inviscid theory based on the acceleration potential for analysing the caudal fin.

Wu (1971a,b) found the efficiency of a flexible plate more compared to that of a rigid plate. Chopra (1974) considered the incompressible flow generated by an oscillating thin rectangular wing with stream-wise and span-wise vortex sheet shed to trail behind the body. The thrust and the propulsive efficiency were characterized with respect to the physical parameters such as aspect ratio, reduced frequency, feathering parameter, and the pitching axis. Chopra (march, 1976) worked out the large amplitude motion of the lunate tail motion using a bound vorticity distribution. He considered both heave and pitch motions such that the effective angle of attack is low. The forces and moments on the airfoil were evaluated based on the theory of impulses. The thrust coefficient and propulsive efficiency were characterized based on the path amplitude, angle of attack and reduced frequency. Chopra (1977) applied the lifting surface theory to small amplitude motion of thin plates with general planform similar to the actual lunate tails of the fast marine animals. The propulsive parameters were characterized with tail aspect ratio, reduced frequency, the feathering parameter, the position of the pitching axis and the curved shape of the leading and trailing edges. The variation of the propulsive parameters were discussed to arrive at an optimal shape.

Katz & Weihs (1978) applied incompressible inviscid irrotational theory to a flexible foil undergoing large amplitude oscillations without inertia effects included. The foil was assumed to be fixed at its leading edge and the flexibility effects were included by allowing the cantilever beam to deform under the fluid dynamic forces. They found that flexibility would increase efficiency by 20%, while causing small decrements in thrust coefficient.

Smith (1995) modeled the effects of flexibility on the aerodynamics of moth wings. They used the aerodynamic panel method for evaluating the potential flow loads on the wing and finite elements for structural model. Liu & Bose (1997) used unsteady inviscid panel method to study the flexible propulsor. The span-wise and chord-wise deformation were predetermined in terms of shape functions. It is shown that passive span-wise flexibility reduces propulsive efficiency, but that propulsive efficiency of these planforms can be increased, over the value for an equivalent rigid foil, by careful control of the phase of the span-wise flexibility relative to other motion parameters.

Jones & Platzer (1997); Tuncer & Platzer (2000); Lewin & Haj-Hariri (2003); Read *et al.* (2003); Young & Lai (2004); Sarkar & Venkatraman (2005) worked on oscillating

rigid airfoils placed in an incompressible viscous flow. They characterized the behavior of the oscillating airfoil with respect to various motion parameters. **Jones & Platzer (1997)** used 2-D inviscid potential analysis coupled with boundary layer algorithm for analysing propulsive characteristics of heaving, pitching and combined heaving-pitching aerofoils. They found that propulsive efficiency increases with decrease in reduced frequency and increase of amplitude of flapping with Strouhal number kept constant. For combined heave-pitch case, the condition of maximum propulsive efficiency is associated with minimum thrust coefficient.

**Tuncer & Platzer (2000)** solved the thin-layer, Reynolds-averaged, compressible Navier-Stokes equation at a Mach number of 0.3 for heaving and flapping airfoil. They characterized the propulsive performance with respect to reduced frequency, amplitude of oscillation, and the phase between heaving and pitching. They found that for attached flows the propulsive efficiency was optimum.

**Read *et al.* (2003)** experimentally studied the effect the of heave amplitude, Strouhal number, angle of attack, and phase angle between heave and pitch on propulsive performance. They found that for large values of Strouhal number which is characterized by distorted angle of attack profile, there is a decrease in thrust value. To get the smooth profile for angle of attack, they introduced higher harmonics of heave motion and found higher thrust values. They found that by introducing pitch bias and having a suddenly started harmonic motion induces substantial amount of transverse forces for maneuvering.

**Lewin & Haj-Hariri (2003)** solved the incompressible viscous flow over heaving elliptic airfoil. They analyzed a heaving airfoil for different values of heave frequency and amplitude. Periodic, aperiodic flow patterns were observed with respect to the various values of Strouhal number and heave frequency. Behaviour of propulsive thrust and efficiency were explained with respect to the leading edge interaction with trailing edge vortex. The high efficiencies are found for a intermediate heaving frequency, whereas in a inviscid analysis the efficiency increases as the heaving frequency decreases.

**Young & Lai (2004)** solved the 2-D unsteady compressible flow for plunging airfoil. The effect of Strouhal number and reduced frequency on the wake structure and propulsive performance was studied. They found leading edge separation to play a major role in evaluating the pressure loads which also depends on the the reduced frequency.

**Sarkar & Venkatraman (2005)** worked on the problem of a heaving airfoil in a viscous flow. They studied asymmetric sinusoidal heave motion, constant heave rate in upstroke and downstroke and sinusoidal pulse train by solving the incompressible viscous flow using a random discrete vortex method. Results were produced for the three cases comparing with that of pure sinusoidal motion both in terms of wake patterns and loads. Asymmetric sinusoidal motion was shown to produce better thrust and lift compared to pure sinusoidal motion.

**Prempraneerach *et al.* (2003); Heathcote *et al.* (2008)** experimentally analyzed chord-wise and span-wise airfoils respectively. **Prempraneerach *et al.* (2003)** experimentally evaluated the propulsive parameters of different airfoils characterised by a non-dimensional flexible parameter. They found that the efficiency of a two dimensional flexible flapping airfoil increases 36% relative to a rigid flapping foil. **Heathcote *et al.* (2008)** experimentally evaluated the effect of span-wise flexibility on the propulsive parameters. They performed experiments on three types of rectangular wing, first being rigid, second being intermediate flexible and third being overly flexible. For intermediate flexible foil, the thrust coefficient and propulsive efficiency are found to be increased whereas for overly flexible foil, the thrust coefficient and propulsive efficiency are low.

**Pederzani & Haj-Hariri (2006)** analysed a heaving flexible airfoil in a viscous flow with inertial effects. The efficiency of the rigid and flexible heaving airfoil is characterised with respect to the density of the membrane as well as reduced frequency. They varied the density of the membrane and studied its effect on the propulsive efficiency and found that lighter airfoils are more efficient then denser airfoils. The airfoil is considered 50% flexible from the trailing edge and the flexibility is modeled as springs attached to the airfoil surface from a rigid support.

**Mittal *et al.* (2006)** studied the hydrodynamics of the pectoral fin, modeled using the finite difference based immersed boundary methodology. Unsteady incompressible Navier-Stokes equation is solved along with continuity equation for the pectoral fin whose

## A numerical study of vortex dynamics of flexible wing propulsors

kinematics is derived from the experimental results of [Lauder et al. \(2006\)](#). Wake topology and hydrodynamic forces are evaluated for the pectoral fin.

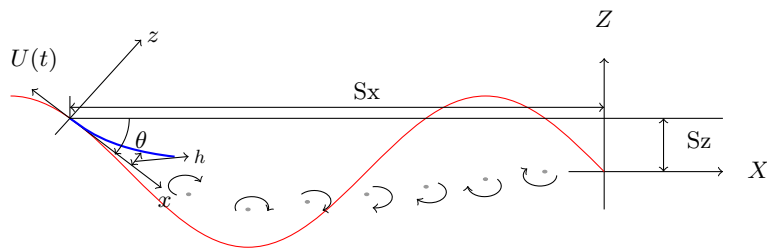
The literature reviewed above points to the fact that flexibility of the foil together with its inertia and its effect on propulsion has not been studied in its entirety. The present work incorporates the inertial loading due to prescribed motion of the foil, and more importantly, includes the flexible body dynamics in computing the unsteady fluid forces. A non-dimensional governing equation of the dynamics of fluid-structure interaction is derived. For structural analysis of the foil, a cantilever beam model is analysed by making the leading edge fixed. An implicit Newmark method is used for computing the structural response of the fluid-structure interaction. The airflow over the foil is modeled as unsteady two dimensional incompressible inviscid flow using discrete vortex elements. An implicit coupling is developed for the fluid-elastic coupling.

## 2. Fluid-structure interaction model

The fluid part is modeled using inviscid airfoil theory as well as incompressible viscous flow. The results for fluid structure interaction is presented in this document uses the inviscid airfoil theory for modeling fluid. Viscous incompressible flow is discussed in Section 2.2 and validation is done for this fluid model for cylinder and plunging elliptical airfoil.

### 2.1. Unsteady inviscid two dimensional airfoil theory

FIGURE 1. Schematic description of model



Consider a thin foil flapping in an inviscid flow, whose amplitude of oscillation is more than its length  $L$ . Initially the airfoil is at the origin of the inertial coordinate system  $X, Z$  and the airfoil moves along a predetermined path  $S(S_x, S_z)$  as shown in Figure 1.

A body fixed coordinate system  $x, z$  for convenience, is defined such that the origin is placed on the path  $S$  and the  $x$ -axis is always tangent to the path. The airfoil shape is defined in  $x - z$  coordinate system by  $h$ , which is considered to be small( $\frac{h}{L} \ll 1$ ). The governing equation for the unsteady incompressible potential flow in the  $x - z$  plane using thin airfoil theory [Katz & Plotkin \(2001\)](#) is given by

$$\nabla^2 \Phi = 0, \quad (2.1)$$

The disturbance potential  $\Phi$  is modeled using the discrete vortex element which inherently satisfies the Kutta condition. The wake is modeled as a distributed set of vortices on a deforming sheet. The boundary conditions for equation 2.1 are that there is no flow through the plate surface  $Z = h(X, t)$  and the disturbance decays far from the plate. The instantaneous strength of the vortex sheet leaving the beam's trailing edge can be calculated by Kelvin's theorem. The fluid dynamic pressures and loads generated by the foil is calculated using unsteady Bernoulli equation.

### 2.2. Unsteady incompressible viscous flow

Immersed boundary method developed by [Mittal et al. \(2008\)](#) is adopted where the mesh grid is kept stationary and the body is moved in the mesh. The boundary condition is applied by sharp interface method. The flow field is solved for the incompressible Navier-Stokes equation and continuity equation. Initially the modified velocity field is obtained by solving the discretized Navier-Stokes equation, where the convection terms are discretised using the Adams-Basforth scheme and diffusion terms are discretised

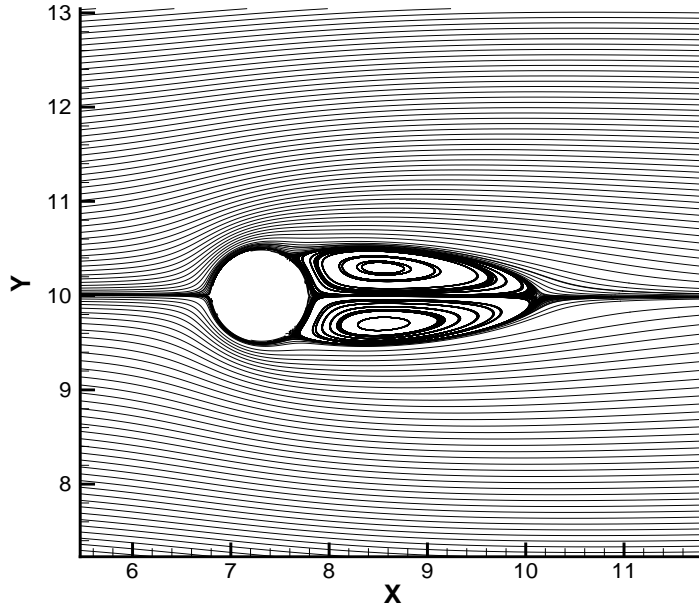


FIGURE 2. Wake patterns after three cycles of heaving motion for flexible foil.

using the Crank-Nicholson scheme. The modified velocity field is corrected using the pressure correction term obtained from pressure poisson equation.

The code developed is in the process of validation. Figure 2 shows the streamline plot of the cylinder for Reynolds number of 40. The coefficient of drag and blob length is calculated to be 1.49 and 2.2, respectively, matches well with the literature (see [Tseng & Ferziger \(2003\)](#)). For unsteady cases, the validation is under process.

### 2.3. Structural Model

A finite element model of foil wing has been constructed, which incorporates the flexibility and mass properties into the structural model. The foil is assumed as a cantilever beam which is fixed at its leading edge. The equation of motion of beam that governs the transverse deformation due to the forces acting on it is

$$m \frac{\partial^2 \eta}{\partial t^2} + \frac{\partial^2}{\partial \zeta^2} \left[ EI \frac{\partial^2 \eta}{\partial \zeta^2} + a_1 \frac{\partial^3 \eta}{\partial^2 \zeta \partial t} \right] = F_f(t) + F_i(t), \quad (2.2)$$

where  $\eta$ ,  $EI$ ,  $m$ ,  $F_f$ ,  $F_i$  are the transverse beam deflection, flexural rigidity, mass per unit length, unsteady hydrodynamic force per unit length, inertial force per unit length respectively. The constant  $a_1$  is the stiffness proportionality factor (see [Clough & Penzein 1993](#)). The non-dimensional form of the above equation is

$$\bar{\omega}_c^2 \frac{\partial^4 \bar{\eta}}{\partial \bar{x}^4} + \bar{a}_1 \bar{\omega}_c^2 \frac{\partial^5 \bar{\eta}}{\partial \bar{x}^4 \partial \tau} + \frac{\partial^2 \bar{\eta}}{\partial \tau^2} = \mu \left( \bar{\Gamma} + \int_0^1 \frac{\partial}{\partial \tau} \bar{\Gamma} d\zeta \right) - \frac{\partial^2 \bar{h}}{\partial \tau^2}. \quad (2.3)$$

The structural response of the cantilever beam model is defined in orthogonal system coordinate system with abscissa along the instantaneous undeflected foil direction. The finite element modeling is done by using the 2D beam element, which uses the Euler-Bernoulli beam theory. Structural response is evaluated by direct integration which uses Newmark's linear acceleration method (see [Cook et al. 2002](#)). The unsteady fluid force due to fluid-structure interaction is obtained from the solution of potential flow field. Fully implicit coupling (see [Pederzani & Haj-Hariri 2006; Bharadwaj et al. 1998; Katz & Weihs 1978](#)) is used for the fluid structure interaction of the flexible airfoil.

# A numerical study of vortex dynamics of flexible wing propulsors

non-dimensional parameter	expression
$\bar{\omega}_c$	$\frac{\sqrt{\frac{E}{mL^4}} L}{U}$
$\bar{\eta}$	$\frac{\eta}{L}$
$\bar{\zeta}$	$\frac{\zeta}{L}$
$\bar{F}$	$\frac{FL}{mU^2}$
$\bar{a}_1$	$\frac{a_1 L}{U}$
$\tau$	$\frac{U}{L} t$
$\mu$	$\frac{\rho L^2}{m}$
$\bar{\Gamma}$	$\frac{\Gamma}{LU}$

### 3. Results and Discussions

Inertial and elastic effects are studied on the hydrofoil exhibiting heaving, pitching and large amplitude undulatory motion. The hydrofoil is fixed at its leading edge and it moves with velocity  $U$  parallel to its length in undeformed state. The thrust coefficient of the foil is

$$C_T = \frac{2}{\rho c U^2} \frac{1}{T} \int_0^T \left( \sum F_x \cos \theta - \sum F_z \sin \theta \right) dt. \quad (3.1)$$

The propulsive efficiency, defined as the ratio of output power to input power, is given by

$$\eta_p = \frac{\frac{1}{T} \int_0^T \left( \sum F_x \cos \theta - \sum F_z \sin \theta \right) \frac{dS_x}{dt} dt}{\frac{1}{T} \int_0^T \left( \sum F_x \sin \theta - \sum F_z \cos \theta \right) \frac{dh}{dt} dt + \int_0^T M_y \frac{d\theta}{dt} dt}. \quad (3.2)$$

Forces  $F_x, F_z$  are the instantaneous forces along the  $x, z$  directions respectively. Moment  $M_y$  is the moment about axis  $y$  due to forces acting on the foil. The non-dimensional parameters mass ratio  $\mu$ , characteristic frequency  $\bar{\omega}_c$  are used to characterize the propulsive performance of the flexible hydrofoil.

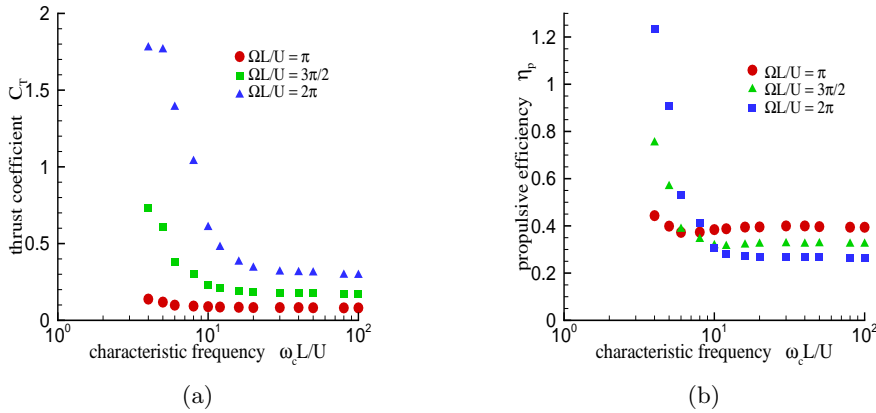


FIGURE 3. Effect of  $\omega_c L/U$  on propulsive parameters,  $\frac{H}{L} = 0.1$ ,  $a_1 L/U = 0.000586$ ,  $\mu = 10$ .

Airfoil in heaving motion is known to produce thrust for all frequencies of heaving where as airfoil in pitching will produce thrust above a certain threshold frequency of

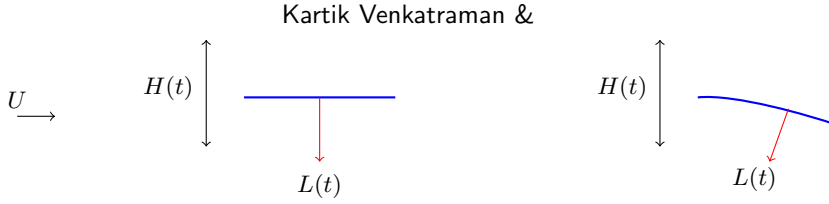


FIGURE 4. Influence of inertia and elasticity on instantaneous lift

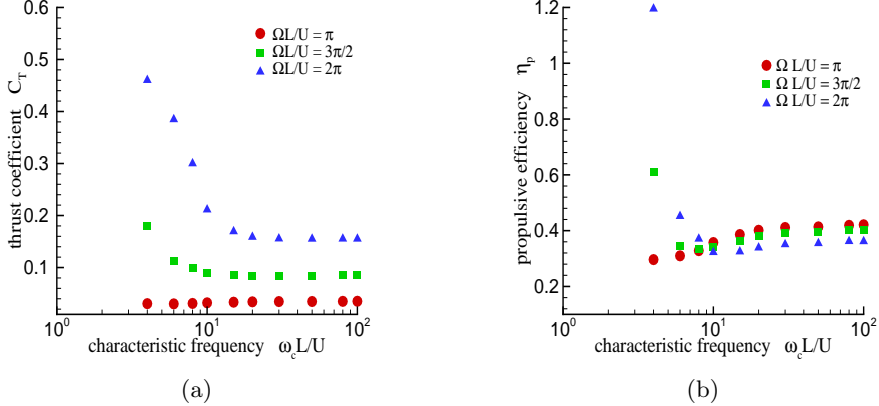


FIGURE 5. Effect of  $\omega_c L/U$  on propulsive parameters,  $\alpha_0 = 5^\circ$ ,  $a_1 L/U = 0.000586$ ,  $\mu = 10$ .

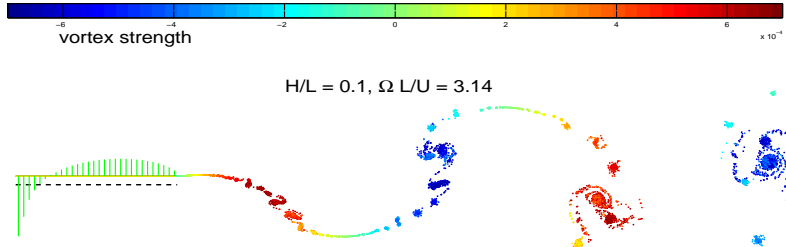


FIGURE 6. Wake patterns after three cycles of heaving rigid foil.

oscillation (see [Garrick 1936](#)). Characteristic frequency  $\omega_c \frac{L}{U}$  represents the flexibility parameter. Higher the value of characteristic frequency the foil is rigid and for lower values of characteristic frequency the foil is flexible. Figure 3(a) shows the variation of the thrust coefficient with respect to  $\frac{\omega_c L}{U}$  for heaving case. The variation of thrust coefficient is shown for different values of  $\frac{\Omega L}{U}$ . As  $\frac{\omega_c L}{U}$  decreases, the thrust coefficient increases. At lower values of  $\frac{\omega_c L}{U}$ , the foil deforms due to the fluid pressure acting on it. The deformed foil produces a force component along the forward velocity direction as shown in the Figure 4. Thus higher thrust coefficient is achieved for lower  $\frac{\omega_c L}{U}$ .

Figure 3(b) shows the variation of efficiency with respect to  $\frac{\omega_c L}{U}$ . As  $\frac{\omega_c L}{U}$  reduces, more thrust is produced at the cost of decreased input effort. Thus higher efficiencies are achieved for lower values of  $\frac{\omega_c L}{U}$ . For higher frequency of heaving, the efficiency is low compared to lower frequency of heaving at larger values of  $\omega_c$ , even though the thrust coefficient is high. This is due to the fact that more effort is spent in high frequency heaving for little improvement in thrust. But as the value of  $\omega_c$  decreases, the higher pressure produces more thrust effect due to deformation of the foil. Thus the efficiencies are more for high frequency heaving at lower values of  $\omega_c$ . Figure 5 shows the effect of character-

## A numerical study of vortex dynamics of flexible wing propulsors

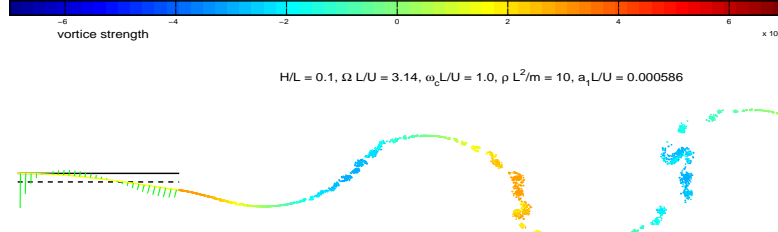


FIGURE 7. Wake patterns after three cycles of heaving flexible foil.

istic frequency on the propulsive performance for pitching case. Similar explanation as that of heaving case holds good for the results shown in Figure 5.

Figure 6 shows the wake patterns at the end of three cycles of heaving motion for a rigid airfoil. Figure 7 shows the wake patterns at the end of three cycles of heaving motion with  $\bar{\omega}_c = 1$ . Clearly we can see the reverse Karman vortex street characterizing thrust producing system. For flexible foil, the strength of the vortex strength in the wake is less compared to the rigid case. And also the vortex roll up is not significant for the flexible foil.

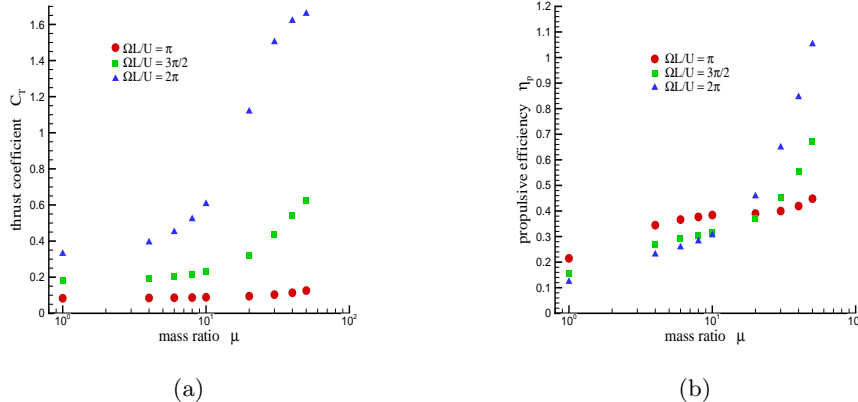


FIGURE 8. Effect of  $\mu$  on propulsive parameters,  $\frac{H}{L} = 0.1$ ,  $a_1 L/U = 0.000586$ ,  $\omega_c L/U = 10$ .

Figure 8(a) shows the variation of thrust coefficient with respect to mass ratio for different plunging frequencies. Figure 8(b) shows the variation of propulsive efficiency with respect to mass ratio for different plunging frequencies. Larger the mass ratio, greater the fluid forces causing the foil to bend. Thus greater propulsive performance is observed for larger values of mass ratio. Figure 9 shows effect of mass ration on propulsive parameters for pitching motion. Similar explanation as that of heaving holds good for pitching also.

### 3.1. Large amplitude undulatory motion

The kinematics of the large amplitude undulatory motion with respect to Figure 1 is given by

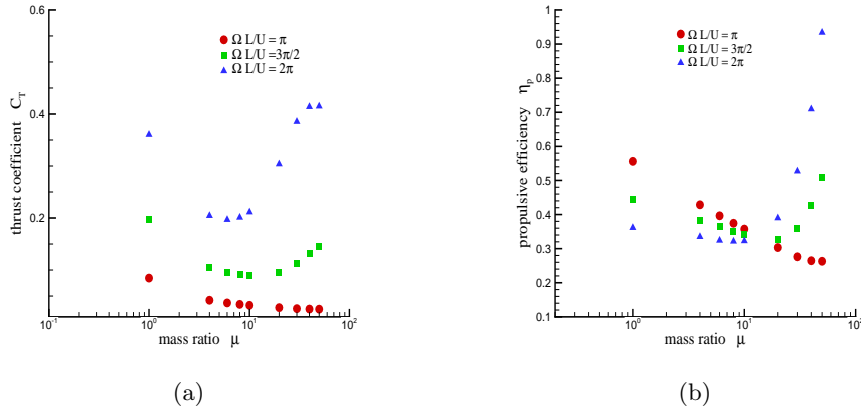


FIGURE 9. Effect of  $\mu$  on propulsive parameters,  $\alpha_0 = 5^\circ$ ,  $a_1 L/U = 0.000586$ ,  $\omega_c L/U = 10$ .

$$\begin{aligned}
 S_x &= -\frac{U}{L}t, \\
 S_z &= \frac{H}{L} \sin(\Omega t), \\
 \alpha &= \alpha_1 + \alpha_0 \sin(\Omega t - \varphi), \\
 \theta &= \tan^{-1} \left[ \frac{dS_z}{dt} / \frac{dS_x}{dt} \right], \\
 \omega &= \frac{d\theta}{dt}.
 \end{aligned} \tag{3.3}$$

In this case the foil follows almost tangent to the sinusoidal path shown in Figure 1 thus maintaining the angle of attack low. Figure 10 shows the effect of characteristic frequency on the propulsive parameters for the large amplitude oscillatory motion. Due to distortion of the flexible foil, the thrust coefficient decreases for the lower values of characteristic frequency. On the contrary the propulsive efficiency increases as the characteristic frequency decreases as the pressure forces orient more towards the thrust direction. But below a certain characteristic frequency, the propulsive efficiency decreases. Due to distortion of the foil, the pressure forces are too low compared to the inertial loads. As the inertial loads contribute to the input of the system dominates the output obtained, there is a dip in the efficiency evaluated at low characteristic frequencies. Figure 11 shows the effect of inertia on the propulsive parameters for the foil undergoing large amplitude undulatory motion. The case where there is no inertia effects, the efficiency is increased with decreased characteristic frequency. When the inertia effects are added, the inertial loads add to the the input of the system. For flexible foil the net output has low value due to distortion of the foil, thus leading to low values of propulsive efficiency.

#### 4. Concluding remarks

Although most of the literature on aquatic propulsion uses potential flow models, the low Reynolds number flow regime, large amplitude motion and high frequency oscillations of the flexible hydrofoil would lead us to believe that viscous flow simulation would be important from the point of flow separation and viscous drag considerations. Viscous flow simulations of flexible hydrofoil using immersed boundary and finite difference (see Mittal *et al.* 2008) based numerical simulation on a cartesian mesh is underway.

#### 5. Acknowledgement

The work presented in this thesis was carried out by Mysa Ravi Chaithanya, a doctoral candidate under the supervision of the author of this report.

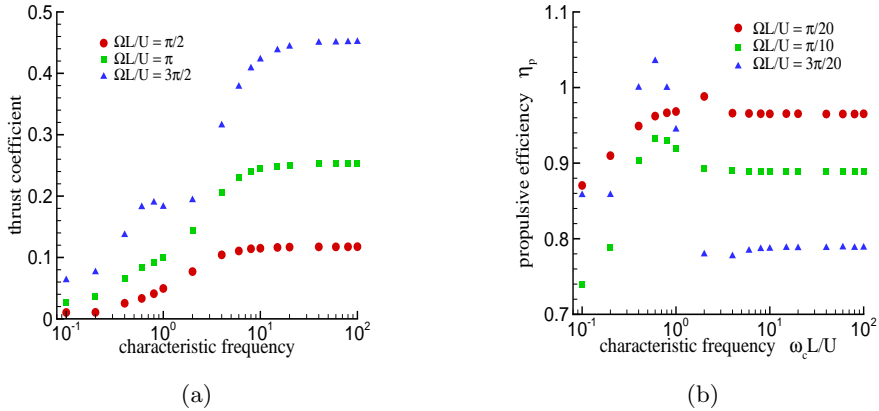


FIGURE 10. Effect of  $\omega_c L/U$  on thrust coefficient,  $\frac{H}{L} = 3$ ,  $\alpha_0 = 5^\circ$ ,  $a_1 L/U = 0.000586$ ,  $\mu = 10$ .

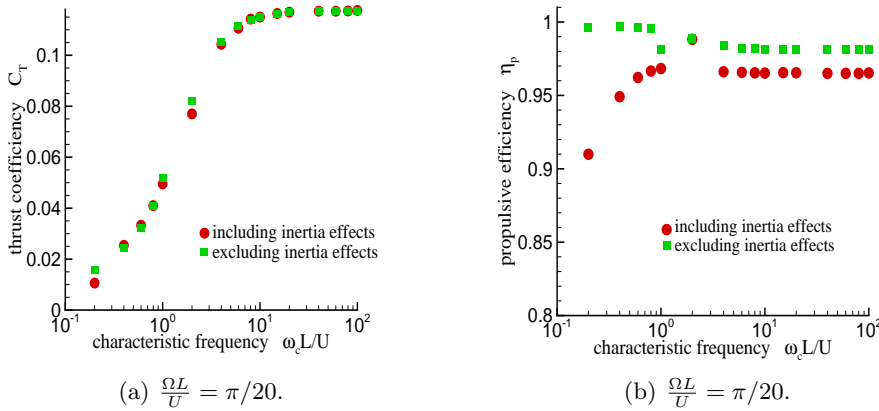


FIGURE 11. Effect of  $\omega_c L/U$  on thrust coefficient,  $\frac{H}{L} = 3$ ,  $\alpha_0 = 5^\circ$ ,  $a_1 L/U = 0.000586$ ,  $\mu = 10$ .

## REFERENCES

- BHARADWAJ, M. K., RAKESH, K. & GURUSWAMY, G. P. 1998 A cfd/csd interaction methodology for aircraft wings. In *Symposium on Multidisciplinary Analysis and Optimization*. AIAA, St. Louis, MO.
- CHOPRA, M. G. 1974 Hydrodynamics of lunate tail swimming propulsion. *Journal of Fluid Mechanics* **64**, 375–391.
- CHOPRA, M. G. 1977 Hydrodynamics of lunate tail swimming propulsion. part 2. *Journal of Fluid Mechanics* **79**, 49–69.
- CHOPRA, M. G. march, 1976 Large amplitude lunate tail theory of fish locomotion. *Journal of Fluid Mechanics* **74**, 161–182.
- CLOUGH, R. W. & PENZEN, J. 1993 *Dynamics of Structures*. McGraw-Hill, Inc.
- COOK, R. D., MALKUS, D. S., PLESCHA, M. E. & WITT, R. J. 2002 *Concepts and Applications of Finite Element Analysis*. Pearson.
- GARRICK, I. E. 1936 Propulsion of a flapping and oscillating airfoil. *NACA Report* **567**.
- HEATHCOTE, S., WANG, Z. & GURSUL, I. 2008 Effect of spanwise flexibility on flapping wing propulsion. *Journal of Fluids and Structures* **24**, 183–199.
- JONES, K. D. & PLATZER, M. F. 1997 Flapping-wing propulsion and power extraction. In *35<sup>th</sup> Aerospace Sciences Meeting and Exhibit*. AIAA, Reno, NV.
- KATZ, J. & PLOTKIN, A. 2001 *Low Speed Aerodynamics*. Cambridge University Press.
- KATZ, J. & WEIHS, D. 1978 Hydrodynamic propulsion by large amplitude oscillation of an airfoil with chordwise flexibility. *Journal of Fluid Mechanics* **88**, 485–497.
- LAUDER, G. V., MADDEN, P. G. A., MITTAL, R., DONG, H. & BOZKURTTAS, M. 2006 Locomotion with flexible propulsors: I. Experimental analysis of pectoral fin swimming in sunfish. *Bioinspiration and Biomimetics* **1** (4), 25–34.
- LEWIN, G. C. & HAJ-HARIRI, H. 2003 Modelling thrust generation of a two-dimensional heaving airfoil in a viscous flow. *Journal of Fluid Mechanics* **51**, 1–29.

- Lighthill, M. J. 1960 Note on the swimming of slender fish. *Journal of Fluid Mechanics* **9**, 305–317.
- Lighthill, M. J. 1970 Aquatic animal propulsion of high hydrodynamical efficiency. *Journal of Fluid Mechanics* **44**, 265–301.
- LIU, P. & BOSE, N. 1997 Propulsive performance from oscillating propulsors with spanwise flexibility. *Proceedings of the Royal Society of London* **453**, 1763–1770.
- MITTAL, R., DONG, H., BOZKURTTAS, M., LAUDER, G. V. & MADDEN, P. 2006 Locomotion with flexible propulsors: II. Computational analysis of pectoral fin swimming in sunfish. *Bioinspiration and Biomimetics* **1** (4), 35–41.
- MITTAL, R., DONG, H., BOZKURTTAS, M., NAJJAR, F. M., VARGAS, A. & LOEBBECKE, A. V. 2008 A versatile sharp interface immersed boundary method for incompressible flows with complex boundaries. *Journal of Computational Physics* **227**, 4825–4852.
- PEDERZANI, J. & HAJ-HARIRI, H. 2006 Numerical analysis of heaving flexible foils in a viscous flow. *AIAA Journal* **88**, 2773–2779.
- PREMPRANEERACH, P., HOVER, F. S. & TRIANTAFYLLOU, M. S. 2003 The effect of chord-wise flexibility on the thrust and efficiency of a flapping foil. In *Proceedings of the 13<sup>th</sup> International Symposium on Unmanned Untethered Submersible Technology*. Autonomous Undersea Systems Institute, Durham New Hampshire.
- READ, D. A., HOVER, F. S. & TRIANTAFYLLOU, M. S. 2003 Forces on oscillating foils for propulsion and maneuvering. *Journal of Fluids and Structures* **17**, 163–189.
- SARKAR, S. & VENKATRAMAN, K. 2005 Numerical simulation of incompressible viscous flow past a heaving airfoil. *International Journal for Numerical Methods in Fluids* **492**, 339–362.
- SMITH, J. C. M. 1995 The effects of flexibility on the aerodynamics of moth wings: Towards the development of flapping wing technology. *Aerospace Sciences Meeting and Exhibit*.
- TSENG, Y. & FERZIGER, J. H. 2003 A ghost-cell immersed boundary method for flow in complex geometry. *Journal of Computational Physics* **192**, 593–623.
- TUNCER, I. H. & PLATZER, M. F. 2000 Computational study of flapping airfoil aerodynamics. *AIAA Journal of Aircraft* **65** (4), 554–560.
- WU, T. Y.-T. 1971a Hydrodynamics of swimming propulsion. Part 1. Swimming of a two-dimensional flexible plate at variable speeds in an inviscid fluid. *Journal of Fluid Mechanics* **46**, 337–355.
- WU, T. Y.-T. 1971b Hydrodynamics of swimming propulsion. Part 2. Some optimum shape problems. *Journal of Fluid Mechanics* **46**, 521–544.
- YOUNG, J. & LAI, J. C. S. 2004 Oscillation frequency and amplitude effects on the wake of a plunging airfoil. *AIAA Journal* **42** (10), 2042–2052.